INTRODUCTION TO RF LINEAR ACCELERATORS

Nicolas Pichoff
CEA/DSM/DAPNIA/SEA, Saclay, France

1. INTRODUCTION

A one-hour lecture on RF linear accelerators (linacs) coupled with a six-hours course (with a smaller group) was proposed to the CAS students. The aim of the lecture was to give to the students an introduction to RF specifies and beam dynamics allowing to get a basic understanding of linacs. The course was dedicated to the high power light ions linacs (protons, H^- or Deuterons) considered in a lot of different projects at that time. This paper deals with the notions introduced in the lecture. Student wanting to learn more about linacs are advised to read books such as [1] and [2].

After a short introduction on applications of RF linacs and their advantages/drawbacks versus circular accelerators, this paper is divided in two parts:

- The *first part* introduces the RF cavity through its basic principle, the notion of RF modes, and the way they are excited either from the RF source or by the beam.
- The *second part* gives useful notions of beam dynamics: The transit time factor, the notion of synchronism, the particle motion in continuous non linear forces (longitudinal dynamics) and periodic linear forces (transverse dynamics). The notion of beam rms properties and the matching in the linac is discussed. The effect of non-linear forces on emittance growth is introduced.

2. WHY RF LINACS

The goal of a particle accelerator is to obtain a *required* beam within the *lowest cost*. By *required*, one means a given particle type, with a given intensity, at a given energy within a given emittance (or brightness) in a given time structure. In the *cost*, the construction as well as the operation costs should be included (including the staff).

Three main competitors fulfilling this goal are: Synchrotrons, cyclotrons and RF linear accelerators (linacs)[1].

The main advantages of linacs are:

- they can handle <u>high current</u> beams (they are not, or less limited by tune shift),

- they can run in <u>high duty-cycle</u> (the beam passes only once at each position),

- they exhibit <u>low synchrotron radiation losses</u> (no dipoles).

The main drawbacks are:

- they require a large number of cavities and need a lot of space,

- the synchrotron radiation damping of light particles (electrons/positrons) cannot be easily used to reduce the beam emittance.

[1] We should not forget electrostatic machines, suitable for low current, low energy beams.

Linacs are therefore mainly used for:

- low energy injectors (where the space-charge force is more important and the duty-cycle is high),
- high intensity/power proton beams (high space-charge level or/and duty cycle),
- new lepton colliders projects at very high energy (no radiation losses).

3. THE RF CAVITIES

The role of a RF cavity is to give energy to the beam. As the RF cost represents usually the major part of the linac costs (except the building), the choice of the RF structure has to be studied very carefully. In this lecture, only the principle of a RF cavity is presented. More detailed information can be found in the CAS sections dedicated to RF [3].

3.1 A standing wave RF cavity

3.1.1 Field calculation

A RF cavity is simply a piece of conductor enclosing an empty volume (generally vacuum). Solutions of Maxwell's equations in this volume, taking into account the boundary conditions on the conductor, allow the existence of electromagnetic fields configurations in the cavity: the *resonant modes*.

Each mode, labelled *n*, is characterized by an electromagnetic field amplitude configuration $\vec{E}_n(\vec{r})/\vec{B}_n(\vec{r})$ oscillating at a RF frequency f_n. The electric field amplitude configuration is solution of the equation:

$$\vec{\nabla}^2 \vec{E}_n + \frac{\omega_n^2}{c^2} \cdot \vec{E}_n = \vec{0}, \tag{1}$$

$\vec{E}_n(\vec{r})$ should satisfy the imposed boundary conditions, and
$\omega_n = 2\pi \cdot f_n$ is the mode pulsation.

The electric field in the cavity is a weighted sum of all the modes:

$$\vec{E}(\vec{r},t) = \sum e_n(t) \cdot \vec{E}_n(\vec{r}) = \sum a_n \cdot e^{j\omega_n t} \cdot \vec{E}_n(\vec{r}). \tag{2}$$

a_n is a complex number,

$e_n(t)$ is the field variation with time, it is solution of [4]:

$$\boxed{\begin{aligned}\ddot{e}_n + \omega_n^2 \cdot e_n = -\frac{\omega_n^2}{\sqrt{\varepsilon\mu}} \cdot \int_S \left(\vec{E} \times \vec{H}_n\right) \cdot \vec{n} \cdot dS \\ + \frac{1}{\varepsilon}\frac{d}{dt}\int_{S'} \left(\vec{H} \times \vec{E}_n\right) \cdot \vec{n} \cdot dS' - \frac{1}{\varepsilon}\frac{d}{dt}\int_V \vec{J}(\vec{r},t) \cdot \vec{E}_n(\vec{r}) \cdot dV\end{aligned}}. \tag{3}$$

$\vec{H}$ is the magnetic induction. It is often used close to the surface in place of $\vec{B}$ as it is macroscopically continuous through the surface (and not $\vec{B}$).

$\vec{J}$ is the current density, of the beam for example.

- The first term on the right hand side of Eq. (3) is an integration over the conductor which is not a perfect conductor. Due to power losses by Joule effects, it can be rewritten as a damping term:

$$-\frac{\omega_n}{Q_{0n}} \cdot \dot{e}_n \,. \tag{4}$$

The calculation of $\boldsymbol{Q_{0n}}$, the *quality factor of the mode*, can be deduced from power losses considerations:

$\boldsymbol{U_n(0)}$ is the energy stored by the *n*-mode at time t=0. For t > 0, no additional power is injected in the cavity. Let's define $\boldsymbol{k(t)}$ as :

$$k(t) = \frac{e_n(t)}{e_n(t=0)} \,. \tag{5}$$

The energy lost per unit time is the power dissipated in the conductor $\boldsymbol{P_n}$:

$$\frac{dU_n(t)}{dt} = -P_n(t) \,. \tag{6}$$

The average power dissipated in the conductor per cycle is proportional to the square of the current density (and thus the magnetic field) close to the surface:

$$P_n = \frac{R_s}{2} \int_S K_n^2 dS = \frac{R_s}{2} \int_S H_n^2 dS \,, \tag{7}$$

$\mathbf{R_s}$ is the surface resistance defined as:

- $R_s = \sqrt{\frac{\mu_0 \pi f_0}{\sigma}}$, for *normal conductors* **(8)**

$\boldsymbol{\sigma}$ is the conductor conductivity ($1/\sigma = 1.7 \cdot 10^{-7}$ Ω.m for copper).

- $R_s \approx R_{res} + 9 \cdot 10^{-5} \frac{f_0^2(GHz)}{T(K)} \exp\left(-1.92 \cdot \frac{T_c}{T}\right)$, for *superconducting niobium* **(9)**

$\boldsymbol{R_{res}}$ is the residual resistance (10^{-9}-10^{-8} Ω) depending on the surface imperfections,

$\boldsymbol{T}$ is the working absolute temperature,

$\boldsymbol{T_c}$ = 9.2 K is the critical temperature.

From equations (5) and (7) can be deduced:

$$P_n(t) = k(t)^2 \cdot P_n(t=0), \tag{10}$$

The stored energy is proportional to the squared of the field:

$$U_i = \frac{\varepsilon_0}{2} \iiint \left\|\vec{E}_i\right\|^2 dv = \frac{1}{2\mu_0} \iiint \left\|\vec{B}_i\right\|^2 dv \ , \tag{11}$$

then:

$$U_n(t) = k(t)^2 \cdot U_n(t=0). \tag{12}$$

Equation **(6)** becomes:

$$\frac{dk^2}{dt} = -\frac{P_n}{U_n} \cdot k^2 = 2 \cdot k\dot{k}, \tag{13}$$

giving:

$$\frac{de_n}{dt} = -\frac{P_n}{2 \cdot U_n} \cdot e_n. \tag{14}$$

A comparison with the damping term written in **(4)** gives:

$$\boxed{Q_{0n} = \frac{\omega_n \cdot U_n}{P_n}}, \tag{15}$$

- In the second term of Eq. (3), the integration is performed over the open surfaces S' and represents the coupling with outside system. This coupling can be divided in 2 contributions:

a) the injected power coming from the power generator through the coupler,

b) an additional damping, which can be represented by an other quality factor $\boldsymbol{Q_{exn}}$ known as the ***external Q,*** corresponding to power losses through the opened surfaces. The coupling can be calculated from the coupler geometry with electromagnetic codes.

$$-\frac{\omega_n}{Q_{exn}} \cdot \dot{e}_n + S_n \cdot e^{j(\omega_{RF} t + \varphi_0)}. \tag{16}$$

$S_n \cdot e^{j(\omega_{RF} t + \varphi_0)}$ is the RF source filling through the coupler.

- The last term of Eq. (3), represents the field excited by the beam, known as the ***beam loading***. It is proportional to the beam intensity:

$$k_n \cdot \underline{I}(t). \tag{17}$$

$\underline{I}(t)$ is a complex number (it has a phase) representing the beam current.

Equation **(3)** can then be modelised by:

$$\boxed{\frac{d^2 e_n}{dt^2} + \frac{\omega_{RF}}{Q_n} \cdot \frac{de_n}{dt} + \omega_n^2 \cdot e_n = S_n \cdot e^{j(\omega_{RF} t + \varphi_0)} + k_n \cdot \underline{I}(t)}, \tag{18}$$

which is the equation of a damped harmonic oscillator in a forced regime.

Q_n is the quality factor of the cavity, with $\frac{1}{Q_n} = \frac{1}{Q_{0n}} + \frac{1}{Q_{exn}}$,

$\tau = 2 \cdot \frac{Q_n}{\omega_{RF}}$ is the cavity filling time.

One notes that both the coupler and the beam can excite some RF modes.

Equation **(18)** is this of an RLC circuit which is often used to modelise the system. A complete study of this model, out of the scope of this lecture, can be found in ref. [4].

Among all these modes, one specific mode, having a field amplitude along longitudinal direction on axis, is used to accelerate the beam. The geometry of the cavity is then calculated to match the frequency of this accelerating mode to the RF frequency. This mode is excited in the cavity through a power coupler whose geometry is calculated and adjusted to transfer electromagnetic energy in the cavity to the beam without reflection (this procedure is called the coupler matching).

3.1.2 Shunt impedances

To first order, one considers that only the accelerating mode is excited in the cavity. The transverse component of the electric field is generally zero on the axis. An expression of the z-component of the field on the axis is then:

$$E_z(s,t) = E_{z0}(s) \cdot \cos(\omega t + \varphi). \tag{19}$$

$E_{z0}(s)$ is the field amplitude.

One defines the *cavity voltage* $\boldsymbol{V_0}$ as:

$$V_0 = \int_{-\infty}^{+\infty} |E_{z0}(s)| \cdot ds. \tag{20}$$

Actually, $q \cdot V_0$ represents the maximum energy (in eV) a particle with charge q could gain if the field was always maximum.

Let $\boldsymbol{P_d}$ be the *power deposition in the cavity*:

$$P_d = \frac{V_0^2}{2 \cdot R}, \tag{21}$$

$\boldsymbol{R}$ is known as the *cavity shunt impedance* and is very useful in cavity design. For an optimum acceleration, it has to be the highest as possible.

Generally, because the electric field is changing with time as the particle transits through the cavity, the maximum energy, $q \cdot V$, that can be gained in the cavity by a particle of charge q is lower than $q \cdot V_0$. One defines the *transit time factor* $\boldsymbol{T}$ as:

$$T = \frac{V}{V_0} \leq 1. \tag{22}$$

It is a corrective factor on the energy gain taking into account the particle transit time in the cavity. It is obviously depending on the particle velocity. A way to calculate it is described in the beam dynamics paragraph.

The *effective shunt impedance* $\boldsymbol{RT^2}$ is then proportional to the ratio between the square of the maximum energy ΔU_{max} that can be gained by the beam and the power lost in the cavity:

$$RT^2 = \frac{\Delta U_{\max}^2}{2P_d}. \quad \textbf{(23)}$$

It is some sort of cavity efficiency and has to be maximum.

The shunt impedance is often used to compare the efficiency of different structure at a given energy. More generally, when the geometry of the structures is different, one extends the preceding definition per unit length to allow for a better comparison.

Let $\boldsymbol{L}$ be the cavity length[2]. The mean cavity electric field $\boldsymbol{E_0}$ is defined as:

$$E_0 = \frac{V_0}{L}. \quad \textbf{(24)}$$

The power deposition per unit length in the cavity $\boldsymbol{P'_d}$ is then:

$$P'_d = \frac{E_0^2}{2 \cdot Z}, \quad \textbf{(25)}$$

$\boldsymbol{Z}$ is the *cavity shunt impedance per unit length*.

The *effective shunt impedance per unit length* $\boldsymbol{ZT^2}$ is then proportional to the ratio between the square of the maximum energy $\Delta U'_{max}$ that can be gained per unit length by the beam and the power lost per unit length in the cavity:

$$ZT^2 = \frac{\Delta U'^2_{\max}}{2P'_d}. \quad \textbf{(26)}$$

As it is depending on the particle velocity, one chooses the structure that maximizes ZT^2 at a given energy. **Figure 1** represents the evolution of the effective shunt impedance per meter for 2 different structures (SDTL and CCL) with different apertures ϕ. The higher the aperture (space available for the beam) the lower is the effective shunt impedance. SDTL structures are more efficient at lower energy and CCL structures are more efficient at higher energy. The optimum transition energy is around 100 MeV for protons.

[2] Due to the cavity fringe field L is often arbitrary defined as the physical length of the cavity.

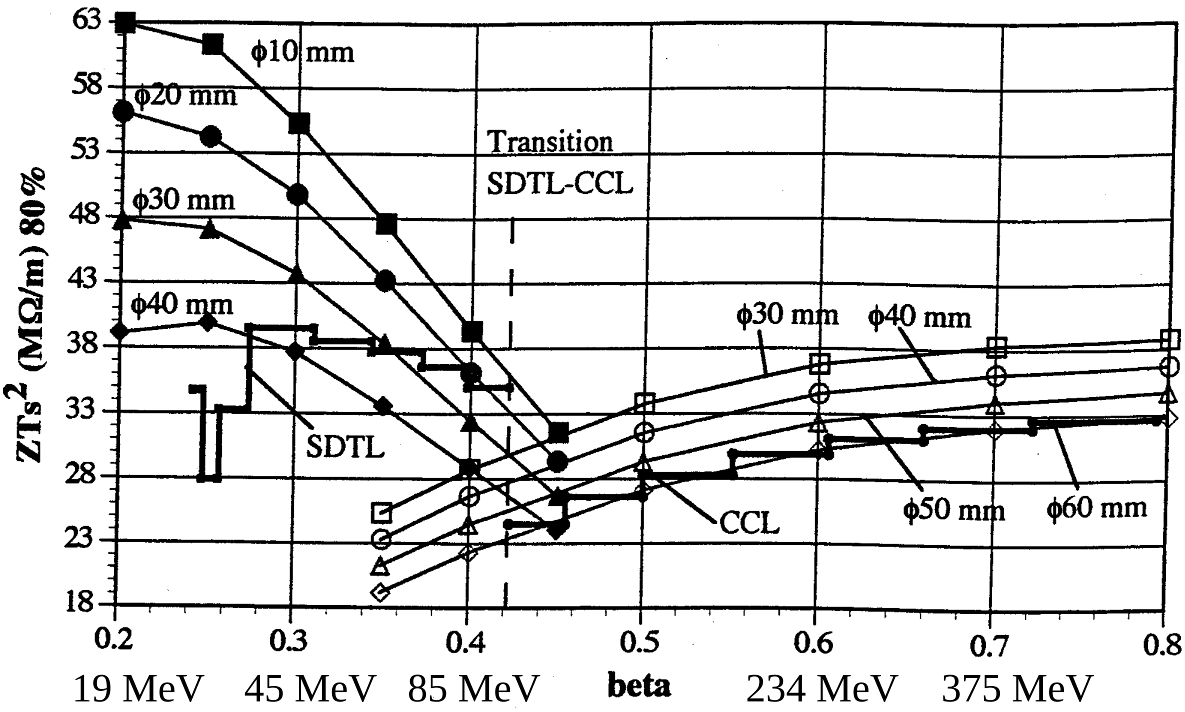

Figure 1 : Effective shunt impedance per meter of different structures

3.2 A travelling wave RF cavity

A travelling wave cavity of cavity is generally used to accelerate ultra-relativistic particles. These cavities have generally two power ports. One from which the power enters, the other, at the other end, to which the power exits (**Figure 2**). The electric field travels through the cavity from the input to the output port. Its phase velocity is adjusted to the beam velocity. The field phase is adjusted to continuously accelerate the beam.

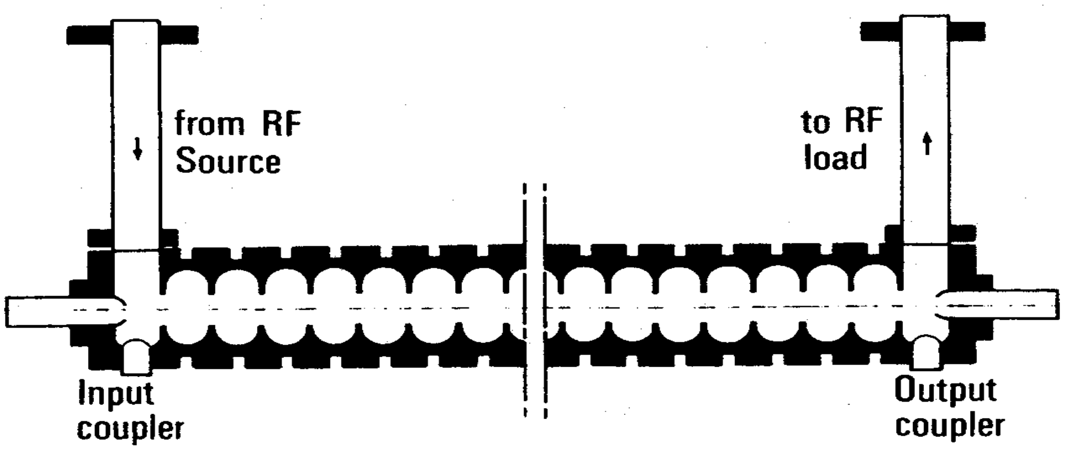

Figure 2 : A travelling wave cavity

The RF phase velocity in empty cavities or wave-guides is usually higher (or equal) than the speed of light in vacuum *c*. As particle velocity cannot excess *c*, the RF phase velocity should be slowed-down to reach the synchronism condition. This can be done by introducing some periodic obstacles into the guide (e.g. an iris-loaded waveguide). The periodic field can then be expanded in a Fourier series, with different wave numbers:

$$Ez(t,z) = \sum_{n=-\infty}^{+\infty} ez_n \cdot \exp\left(j \cdot (\omega t - k_n z)\right). \qquad \textbf{(27)}$$

ez_n are the ***space harmonic*** amplitudes,
k_n are the space harmonic wave numbers,

$$k_n = k_0 + \frac{2\pi n}{d}, \qquad \textbf{(28)}$$

d is the obstacle period, and
$\boldsymbol{k_0}$ is the guide wave number.

The phase velocity $\boldsymbol{v_n}$ of space-harmonic number *n* is:

$$v_n = \frac{\omega}{k_n}. \qquad \textbf{(29)}$$

Particle whose velocity is close to the phase velocity of one space harmonic exchanges energy with it. Otherwise, the average effect is null.

A complete calculation of these insertion obstacles as well as a large bibliography can be found in ref. [5]. This kind a travelling wave accelerating structure is mainly used to accelerate ultra relativistic electrons.

Moreover, this model of a travelling wave acceleration is often used to simplify the calculation of the longitudinal motion equations (even for acceleration with standing wave cavities).

4. ELEMENTS OF BEAM DYNAMICS

4.1 The transit time factor and the particle synchronous phase

A cavity has a finite length ***L***. $\boldsymbol{s_0}$ is the cavity input abscissa. $\boldsymbol{E_z(s)}$ is the amplitude of the electric field longitudinal component on axis.

The energy[3] gained by a charged particle <u>on axis</u> in the cavity is:

$$\Delta W = \int_{s_0}^{s_0+L} qE_z(s) \cdot \cos(\phi(s)) \cdot ds, \qquad \textbf{(30)}$$

q is the particle charge,

$\boldsymbol{\phi(s)}$ is the cavity RF phase when the particle is at abscissa s. It is defined as:

$$\phi(s) = \phi_0 + \frac{\omega}{c} \int_{s_0}^{s_0+s} \frac{ds'}{\beta_z(s')} \qquad \textbf{(31)}$$

$\boldsymbol{\phi_0} = \phi(s_0)$ is the RF phase when the particle enters the cavity.

[3] This is actually the longitudinal energy, but we can consider that there is no transverse field on cavity axis.

Writing $\phi(s) = \phi(s) + (\phi_s - \phi_s)$, $\boldsymbol{\phi_s}$ being an arbitrary phase and using trigonometric relationships, one gets for the energy gain:

$$\Delta W = \cos\phi_s \cdot \int_{s_0}^{s_0+L} qEz(s)\cdot\cos(\phi(s)-\phi_s)\cdot ds - \sin\phi_s \cdot \int_{s_0}^{s_0+L} qEz(s)\cdot\sin(\phi(s)-\phi_s)\cdot ds. \qquad \textbf{(32)}$$

By defining ϕ_s such as: $\int_{s_0}^{s_0+L} qEz(s)\cdot\sin(\phi(s)-\phi_s)\cdot ds = 0$,

Giving the definition of the ***synchronous phase*** $\boldsymbol{\phi_s}$:

$$\boxed{\phi_s = \arctan\left(\frac{\int_{s_0}^{s_0+L} Ez(s)\cdot\sin(\phi(s))\cdot ds}{\int_{s_0}^{s_0+L} Ez(s)\cdot\cos(\phi(s))\cdot ds}\right)}, \qquad \textbf{(33)}$$

one finally gets:

$$\boxed{\Delta W = \left(q\int_{s_0}^{s_0+L} |Ez(s)|\cdot ds\right)\cdot T\cdot\cos\phi_s = qV_0\cdot T\cdot\cos\phi_s}, \qquad \textbf{(34)}$$

with:

$$\boxed{T = \frac{1}{V_0}\int_{s_0}^{s_0+L} Ez(s)\cdot\cos(\phi(s)-\phi_s)\cdot ds}. \qquad \textbf{(35)}$$

T is known as the ***transit time factor***. It depends on the particle initial velocity as well as on the field amplitude. It can be noticed that this definition does not make any assumption on the field shape (no symmetry) resulting from a slightly different synchronous phase definition which can be found in literature (which is often taken as the RF phase when the particle reaches the mid-cavity). When the velocity gain in the cavity is much lower than the input particle velocity, *T* depends only on the velocity and can be easily tabulated.

The calculation of *T* with formula **(35)** is sometimes difficult to do as ϕ_s has to be known. In fact, *T* does not depend on ϕ_s when the velocity gain is small and an other formula (a little bit more difficult to understand physically) can be used:

$$\boxed{T = \frac{1}{V_0}\left|\int Ez(s)\cdot e^{j\phi(s)}\cdot ds\right|}. \qquad \textbf{(36)}$$

4.2 Notion of Synchronism

A linac is designed such that a theoretical particle, called the *synchronous particle,* enters successively on axis the RF cavities with a predefined RF phase in order to get a required energy gain. This very important notion of synchronism allows understanding the efficiency as well as the stability of the linacs.

Particles can be accelerated with travelling waves as well as standing waves structures.

4.2.1 Acceleration with travelling waves

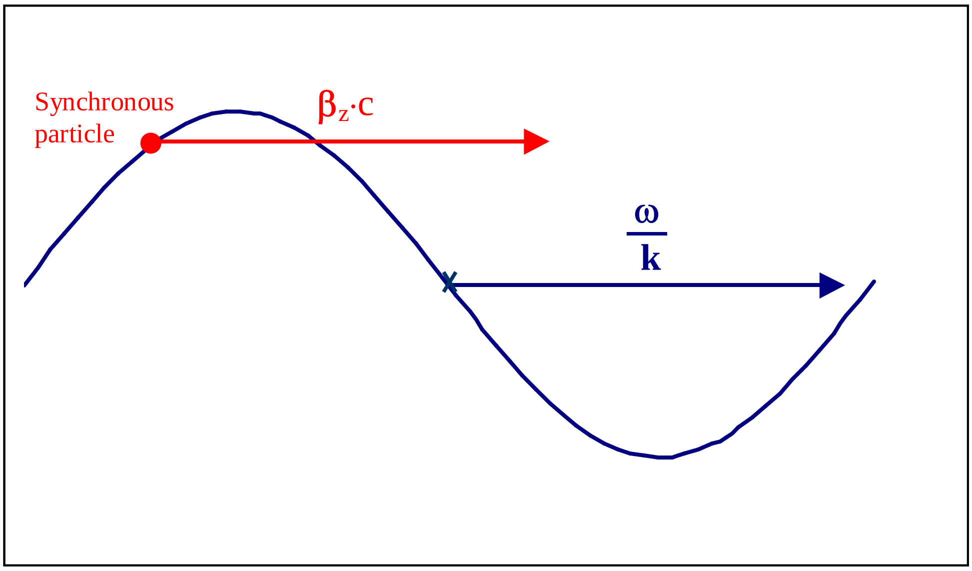

Figure 3: Particle accelerated by a travelling wave

The on-axis RF accelerating field can be written as:

$$E_z(z,t) = E_0 \cdot \cos(\omega t - kz), \tag{37}$$

$\boldsymbol{\omega}$ is the RF pulsation,

$\boldsymbol{k}$ is the RF wave number.

The synchronism condition is reached when the particle longitudinal velocity equals the RF phase velocity:

$$\beta_z c = \frac{k}{\omega}. \tag{38}$$

$\boldsymbol{c}$ is the speed of light in vacuum,

$\boldsymbol{\beta_z}$ is the reduced longitudinal velocity of the synchronous particle. It can be noticed that when the *paraxial approximation*[4] is used, β_z is replaced by β, the reduced total speed of the particle.

4.2.2 Standing waves

In most linacs, the beam is accelerated with RF cavities or gaps operating in standing wave conditions. A RF power, produced by one or many RF sources, is introduced through a coupler in a resonant cavity exciting the wanted standing wave accelerating mode. The cavity shape has been calculated and adjusted to match the accelerating mode to the power-supply frequencies and to throw the other modes frequencies far from the RF one.

[4] as $\beta = \beta_z \cdot \sqrt{1 + x'^2 + y'^2}$, paraxial approximation occurs when x' << 1 and y' << 1.

As a first step, let's assume a set of thin independently phased RF cavities along the beam path (**Figure 4**).

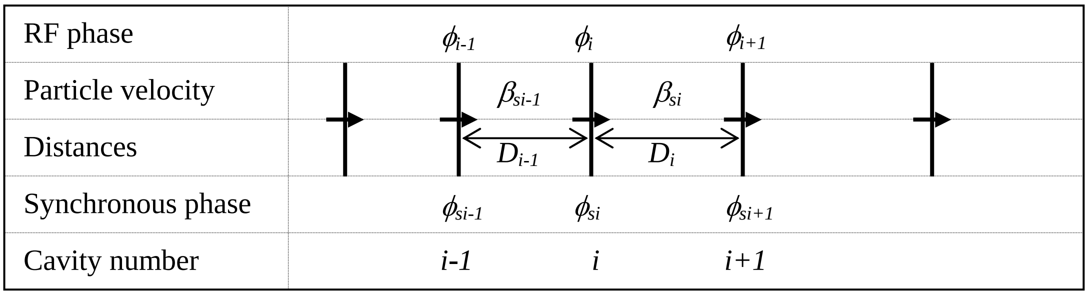

Figure 4 : A set of independently phased cavity

$\boldsymbol{\phi_i}$ is the absolute RF phase in the i[th] cavity when t=0 (t=0 has been arbitrarily defined),

$\boldsymbol{\beta_{si}}$ is the synchronous particle reduced velocity at the i[th] cavity output,

$\boldsymbol{\phi_{si}}$ is the RF synchronous phase of the i[th] cavity of the synchronous particle[5],

$\boldsymbol{D_i}$ is the distance between the i[th] and the i+1[th] cavities.

The synchronism condition is reached when:

$$\phi_{si+1} - \phi_{si} = 2\pi \cdot \frac{D_i}{\beta_{s\,i}\lambda} + \phi_{i+1} - \phi_i + [2\pi n]. \tag{39}$$

$\lambda = \dfrac{c}{f}$ is the RF wavelength.

One observes that the synchronism condition does not depend on the RF field amplitude. It has a non intuitive consequence : an increase of the accelerating field amplitude in the cavities without phase change does not induce an increase of the synchronous particle final energy but a change of the synchronous phase fulfilling the synchronism condition.

Two different kinds of structures exist:

- The coupled cavity structures where the phase between cavities is fixed. The synchronism condition is achieved by adjusting the distance between the cavities.

In a Drift Tube Linac (DTL), for example, the phase difference between the cells is fixed (=2π). The distance between cells is then calculated to have:

$$D_i = \left(\frac{\phi_{si+1} - \phi_{si}}{2\pi} + 1 \right) \cdot \beta_{s\,i}\lambda \tag{40}$$

- The independent cavity structures where the distance between cavities is fixed. The synchronism condition is then achieved by adjusting the phase difference between the cavities.

[5] Don't confuse the *synchronous-particle phase*, which is the phase of the synchronous particle in a cavity and a *particle synchronous-phase* which is the synchronous phase of a particle (whatever it is) in a cavity.

In a Superconducting Cavity Linac (SCL), for example, the distance between cavities is fixed by the cryogenics mechanics. The phase difference between cavities is then calculated to have:

$$\phi_{i+1} - \phi_i = \phi_{si+1} - \phi_{si} - 2\pi \cdot \frac{D_i}{\beta_{s\,i}\lambda} + [2\pi n]. \tag{41}$$

4.3 Particle motion in electromagnetic fields

4.3.1 Basis

Electromagnetic field can be divided in 2 contributions:

- The electric field: $\vec{\boldsymbol{E}}$,
- The magnetic field: $\vec{\boldsymbol{B}}$.

The intensity of these contributions depends on the referential where they are expressed.

The motion equation of a particle of charge q in these fields is:

$$\frac{d\vec{p}}{dt} = q \cdot \left(\vec{v} \times \vec{B} + \vec{E}\right). \tag{42}$$

$\vec{p}$ is the momentum of the particle, $\vec{v}$ is its velocity.

Lets call ***s*** the abscissa of the beam in the linac path (rather than z to avoid any confusion with the particle longitudinal position in the bunch), the motion equation can be rewritten:

$$\frac{d\vec{p}}{ds} = q \cdot \frac{\vec{v} \times \vec{B} + \vec{E}}{v_z}, \tag{43}$$

v_z is the particle longitudinal velocity.

A projection on Cartesian axis[6] (x, y, z) gives:

$$\boxed{\begin{cases} \dfrac{d\gamma\beta_x}{ds} = \dfrac{q}{mc} \cdot \left(y'B_z - B_y + \dfrac{E_x}{v_z} \right) = \dfrac{d\gamma\beta_z x'}{ds} \\ \dfrac{d\gamma\beta_y}{ds} = \dfrac{q}{mc} \cdot \left(B_x - x'B_y + \dfrac{E_y}{v_z} \right) = \dfrac{d\gamma\beta_z y'}{ds} \\ \dfrac{d\gamma\beta_z}{ds} = \dfrac{q}{mc} \cdot \left(x'B_y - y'B_x + \dfrac{E_z}{v_z} \right) \end{cases}} \tag{44}$$

$x' = \dfrac{dx}{ds} = \dfrac{p_x}{p_z} = \dfrac{\beta_x}{\beta_z}$ and $y' = \dfrac{dy}{ds} = \dfrac{p_y}{p_z} = \dfrac{\beta_y}{\beta_z}$ are the slopes of the particle,

[6] In general, *x* and *y* play the same role in a linac (in contrary of in circular accelerator).

$\beta_w = \frac{v_w}{c}$, the reduced velocity w-component, *w* being *x*, *y* or *z*, v_w being the particle velocity *w* component,

m and *q* are respectively the rest mass and the charge of the particle,

c is the speed of light.

One clearly observes that longitudinal and transverse motions are coupled. However, for an easier understanding, and because the coupling is often very weak, the longitudinal and the transverse motions are usually treated as uncoupled, the longitudinal velocity v_z variations being considered apart. To uncouple the transverse and longitudinal motions, the ***paraxial approximation*** has to be done.

4.3.2 Paraxial approximation

The *paraxial approximation* consists in assuming that $x'^2 + y'^2 << 1$.

Its natural consequence is :

$$\beta_z = \beta \cdot \sqrt{1 + x'^2 + y'^2} \approx \beta . \qquad \textbf{(45)}$$

For $x' < 100$ mrad and $y' < 100$ mrad, the error on β (or β_z) is lower than 1%!!!

This approximation is very good at high energy where the beam divergence is small, but is more difficult to justify at very low energy!

4.3.3 Energy gain calculation

From Eqs. **(44)**, one can easily obtain the energy gain:

$$\frac{d\gamma}{ds} = \beta_z \left(x' \cdot \frac{d\gamma\beta_x}{ds} + y' \cdot \frac{d\gamma\beta_y}{ds} + \frac{d\gamma\beta_x}{ds} \right), \qquad \textbf{(46)}$$

giving :

$$\boxed{\frac{d\gamma}{ds} = \frac{q}{mc^2} \cdot \left(x'E_x + y'E_y + E_z \right)}. \qquad \textbf{(47)}$$

One finds the well-known result that the only electric field contributes to energy gain.

4.4 Longitudinal particle dynamics (motion in non linear force)

4.4.1 The longitudinal variables

The variables generally used to describe the longitudinal particle motion, as a function of *s*, are:

ϕ, the absolute particle phase, calculated from the RF frequency, with $\phi = 0$ arbitrary chosen.

W, the particle kinetic energy[7].

[7] This is really a "longitudinal" particle property only in paraxial approximation !!

The evolution of these variables with *s* is given by the equations:

$$\begin{cases} \dfrac{d\phi}{ds} = \dfrac{\omega_{rf}}{\beta_z c} = \dfrac{2\pi}{\beta \cdot \lambda_{rf} \cdot \sqrt{1 - x'^2 - y'^2}} \\ \dfrac{dW}{ds} = q \cdot \left(x' E_x(s,\phi,r) + y' E_y(s,\phi,r) + E_z(s,\phi,r) \right) \end{cases} \quad \textbf{(48)}$$

Applying these equations to the synchronous particle, one gets:

$$\begin{cases} \dfrac{d\phi_s}{ds} = \dfrac{2\pi}{\beta_s \cdot \lambda_{rf}} \\ \dfrac{dW_s}{ds} = q \cdot E_z(s,\phi_s,0) \end{cases} \quad \textbf{(49)}$$

Let us define the reduced phase and energy variables for each particle:

$$\begin{cases} \varphi = \phi - \phi_s \\ w = W - W_s \end{cases} \quad \textbf{(50)}$$

Late particles have a positive φ.

The motion equations with these new variables become:

$$\begin{cases} \dfrac{d\varphi}{ds} = \dfrac{2\pi}{\lambda_{rf}} \cdot \left(\dfrac{1}{\beta \cdot \sqrt{1 - x'^2 - y'^2}} - \dfrac{1}{\beta_s} \right) \\ \dfrac{dw}{ds} = q \cdot \left(x' E_x(s,\phi,r) + y' E_y(s,\phi,r) + E_z(s,\phi,r) - E_z(s,\phi_s,0) \right) \end{cases} \quad \textbf{(51)}$$

When the beam is accelerated by a standing wave cavity structure, a synchronous particle enters successive cavities receiving a strong energy gain, separated by long drift spaces where no acceleration occurs. In order to ease the understanding of the physics, this periodic acceleration scheme can be replaced by a continuous acceleration one. This scheme consists in assuming that the beam is accelerated by a travelling wave propagating at the same speed than that of the synchronous particle. This scheme allows a mathematical resolution of the dynamics equations[8] with the electric field that does not depend on *s*.

4.4.2 The electric field model

The electric field, which is generally a function of *s*, is then chosen constant. The field amplitude of the travelling wave is $\boldsymbol{E_0 T}$ (mean electric field) on axis. $\boldsymbol{E_0}$ is defined as the potential gain of one

[8] Equations are smoothed for analytic solutions, then quantified for a numerical solution!

cavity V_0 divided by the distance between the centres of consecutive cavities. The transit time factor ***T*** has been included to take into account the variable efficiency of the acceleration in standing wave cavities with the particle velocity.

The on-axis electric field longitudinal component becomes:

$$E_z(s,\varphi,r=0) = E_0 T \cdot \cos(\varphi + \phi_{s0}), \tag{52}$$

$\boldsymbol{\phi_{s0}}$ being the RF synchronous phase of the synchronous particle.

The energy gain per meter of the synchronous particle is then:

$$G = qE_0 T_s \cdot \cos\phi_{s0}. \tag{53}$$

$\boldsymbol{T_s}$ is the transit time factor of the synchronous particle.

Let's assume an *axisymmetric accelerating field*, the off-axis electric field longitudinal component can be written :

$$E_z(s,\phi,r) = E_0 T \cdot R(r) \cdot \cos(\varphi + \phi_{s0}), \tag{54}$$

r being the radial position of the particle,

R(*r*) is expressing the radial evolution of the electric field longitudinal component. It can usually be written as $R(r) = 1 + O(r^2)$. Close to the axis, Bessel function, solution of the Maxwell equations in axisymmetric geometry in vacuum, can be used to expressed *R*(*r*) [2][6], but far from the axis, the cavity geometry has a strong influence through the boundary conditions. The radial position (*r*) can be replaced by (*x*,*y*) if the cavity is not axisymmetric. Some authors include the variation of the field with *r* in the transit time factor: *T(r)*

From the relationship $\vec{\nabla} \cdot \vec{E} = 0$ and remarking that the electric field transverse component is zero on axis, one gets the electric field transverse component:

$$\begin{aligned} E_r(s,\varphi,r) &= -\frac{1}{r} \cdot \int_0^r \frac{\partial E_z(s,\varphi,r)}{\partial s} \cdot r \cdot dr \\ &= -\frac{1}{r} \cdot \frac{E_0 T}{\beta_s \lambda} \cdot \sin(\varphi + \phi_{s0}) \cdot \int_0^r R(r) \cdot r \cdot dr \end{aligned} \tag{55}$$

The electric field radial component can be written:

$$E_r(s,\varphi,r) = -\frac{E_0 T}{\beta_s \lambda} \cdot \sin(\varphi + \phi_{s0}) \cdot \left(\frac{r}{2} + O(r^3)\right). \tag{56}$$

Three assumptions should be done to decouple the longitudinal motion from the transverse one:

- In general, we can assume: $\frac{r}{2} + O(r^3) << \beta_s \lambda$. As (*x'*, *y'*) << 1, and the contribution of the transverse electric field to the energy gain can be usually neglected in equation **(51)**:

$$x'E_x + y'E_y << E_z - E_{zs}\,. \qquad \textbf{(57)}$$

- Generally, the *paraxial assumption* holds, and we consider:
-

$$x'^2 + y'^2 << 1\,. \qquad \textbf{(58)}$$

- Finally, we can assume that the longitudinal field does not depend on the radial position *r*, by taking:
-

$$R(r) \approx 1\,. \qquad \textbf{(59)}$$

4.4.3 The equations of motion

Using these assumptions, Eqs. (51) become:

$$\begin{cases} \dfrac{d\varphi}{ds} = -\dfrac{2\pi}{\lambda}\left(\dfrac{1}{\beta(s)} - \dfrac{1}{\beta_s(s)}\right), \\ \dfrac{dw}{ds} = -q \cdot E_0 T \cdot \left(\cos\phi_{s0} \cdot (1-\cos\varphi) + \sin\phi_{s0} \cdot \sin\varphi\right). \end{cases} \qquad \textbf{(60)}$$

which is in fact the equation of motion for on-axis particles.

Moreover, a small longitudinal velocity dispersion assumption can be done:

$$\frac{1}{\beta} - \frac{1}{\beta_s} = \delta\beta^{-1} << \frac{1}{\beta_s}\,, \qquad \textbf{(61)}$$

and a *first order development* around the synchronous velocity gives: $\delta\beta^{-1} = -\dfrac{w}{(\beta_s\gamma_s)^3 \cdot mc^2}$.

If one considers that the transit-time factor does not depends on the beam particles energy:

$$T(w) = T_s\,, \qquad \textbf{(62)}$$

Equations (60) become:

$$\begin{cases} \dfrac{d\varphi}{ds} = -2\pi \cdot \dfrac{w}{(\beta_s\gamma_s)^3 \cdot mc^2 \cdot \lambda} = \dfrac{\partial H_{\phi w}}{\partial w} \\ \dfrac{dw}{ds} = -q \cdot E_0 T_s \cdot \left(\cos\phi_{s0} \cdot (1-\cos\varphi) + \sin\phi_{s0} \cdot \sin\varphi\right) = -\dfrac{\partial H_{\phi w}}{\partial\varphi} \end{cases} \qquad \textbf{(63)}$$

As φ and *w* are canonical variables with the independent variable *s*, a Hamiltonian $\boldsymbol{H_{\varphi w}}$ has been used to describe the particle motion:

$$H_{\varphi w} = -\frac{2\pi}{(\beta_s\gamma_s)^3 \cdot mc^2 \cdot \lambda} \cdot \frac{w^2}{2} - q \cdot E_0 T_s \cdot R(r) \cdot \left(\sin\phi_{s0} \cdot (\cos\varphi - 1) + \cos\phi_{s0} \cdot (\sin\varphi - \varphi)\right). \quad \textbf{(64)}$$

In the phase space (φ, w), particles are following curves for which: $H_{\phi w}$ = Cst. They are represented on **Figure 5** for on-axis particle. On **Figure 5.a)**, $\beta_s\gamma_s$ = Cst, whereas on **Figure 5.b)**, an adiabatic acceleration ($\beta_s\gamma_s \neq$ Cst) is added and the bucket turns into the well-known *golf club* shape.

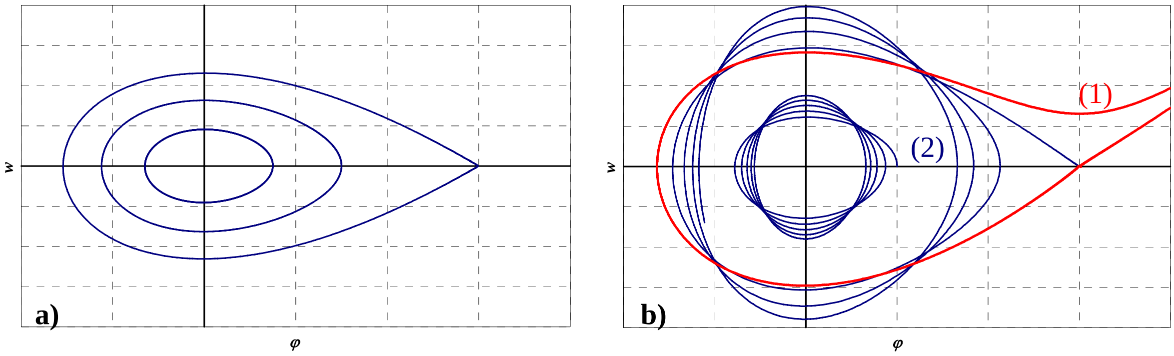

Figure 5 : Particle trajectories in longitudinal phase-space

a) $\beta_s\gamma_s$ = Cst,

b) Adiabatic acceleration : the *golf club* represents the input acceptance (in red, (1)). In blue (2) are the trajectories of 2 particles. They exhibit the damping of the phase oscillation amplitude with acceleration.

A particle entering the cavity later than the synchronous particle gets a larger energy gain. A particle entering the cavity in advance (called the early particle) gets a smaller energy gain.

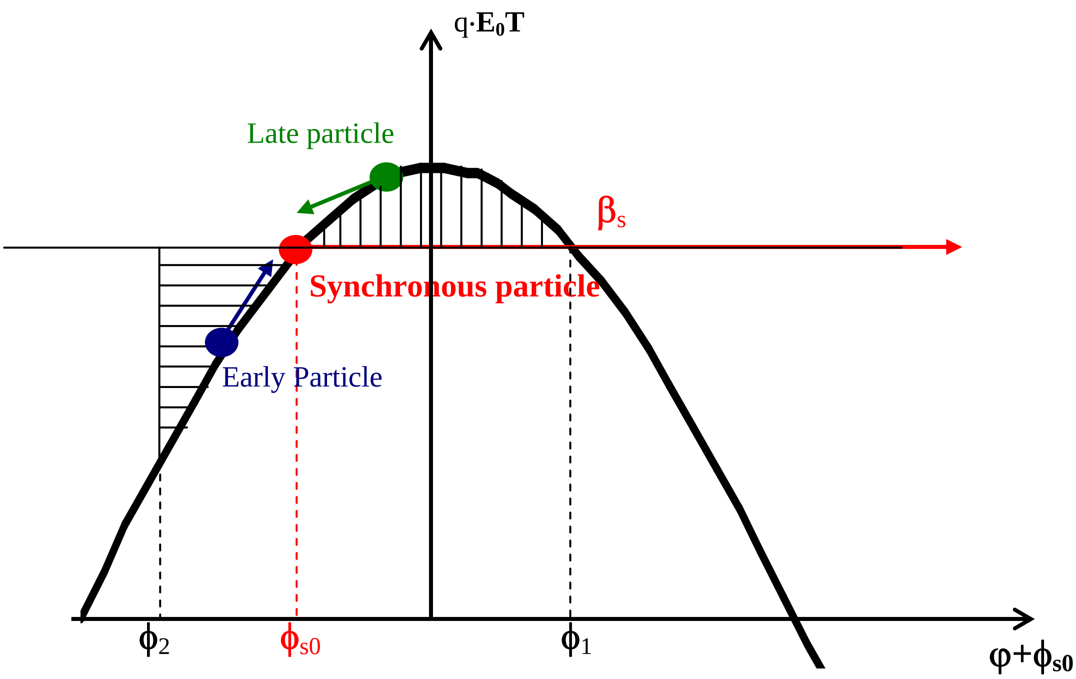

Figure 6 : Energy gain - Synchronous particle

The synchronous phase of the synchronous particle is a stable point situated between $-\pi/2$ and 0[9].

The choice of the synchronous phase delimits a phase acceptance:

- The higher limit ϕ_1 is the phase for which a late particle gets the same energy gain as the synchronous particle:
-

$$\phi_1 = -\phi_{s0} \qquad \Rightarrow \qquad \varphi_1 = -2 \cdot \phi_{s0} \tag{65}$$

- At the lower limit ϕ_2, the confinement potential equals the potential at the higher limit (ϕ_1). As the potential is the integral of the force, ϕ_2 is the phase for which the horizontally hatched surface (on **Figure 6**) equals the vertically hatched one. It can be calculated from the Hamiltonian given in Eq. (64):
-

$$H_{\varphi w}(\varphi = \phi_2 - \phi_{s0}, w = 0) = H_{\varphi w}(\varphi = \phi_1 - \phi_{s0}, w = 0). \tag{66}$$

ϕ_2 is solution of :

$$(\sin\phi_2 - \phi_2 \cos\phi_{s0}) + (\sin\phi_{s0} - \phi_{s0}\cos\phi_{s0}) = 0\ . \tag{67}$$

- The choice of the synchronous phase determines also the energy acceptance ***ΔE*** corresponding to the difference between the potential energy of a particle with a phase ϕ_1 and the synchronous particle. It can be also calculated from the Hamiltonian given in Eq.(64):
-

$$H_{\varphi w}(\varphi = 0, w = \Delta E) = H_{\varphi w}(\varphi = \phi_1 - \phi_{s0}, w = 0). \tag{68}$$

giving:

$$\Delta E = 2 \cdot qE_0 T(\phi_{s0}\cos\phi_{s0} - \sin\phi_{s0}). \tag{69}$$

$$\Delta E = \left(\frac{(\beta_s\gamma_s)^3 \cdot \lambda \cdot mc^2}{\pi} \cdot 2 \cdot qE_0 T(\phi_{s0}\cos\phi_{s0} - \sin\phi_{s0}) \right)^{\frac{1}{2}}. \tag{70}$$

The acceptance area in the phase-energy space is called the ***bucket***, its limit is called the ***separatrix***. The energy acceptance *ΔE* and the phase ϕ_2 are represented as a function of the synchronous phase on **Figure 7**.

9 For positively charged particle, as for negative charged one it depends on convention (is $qE_0>0$ or $E_0>0$?).

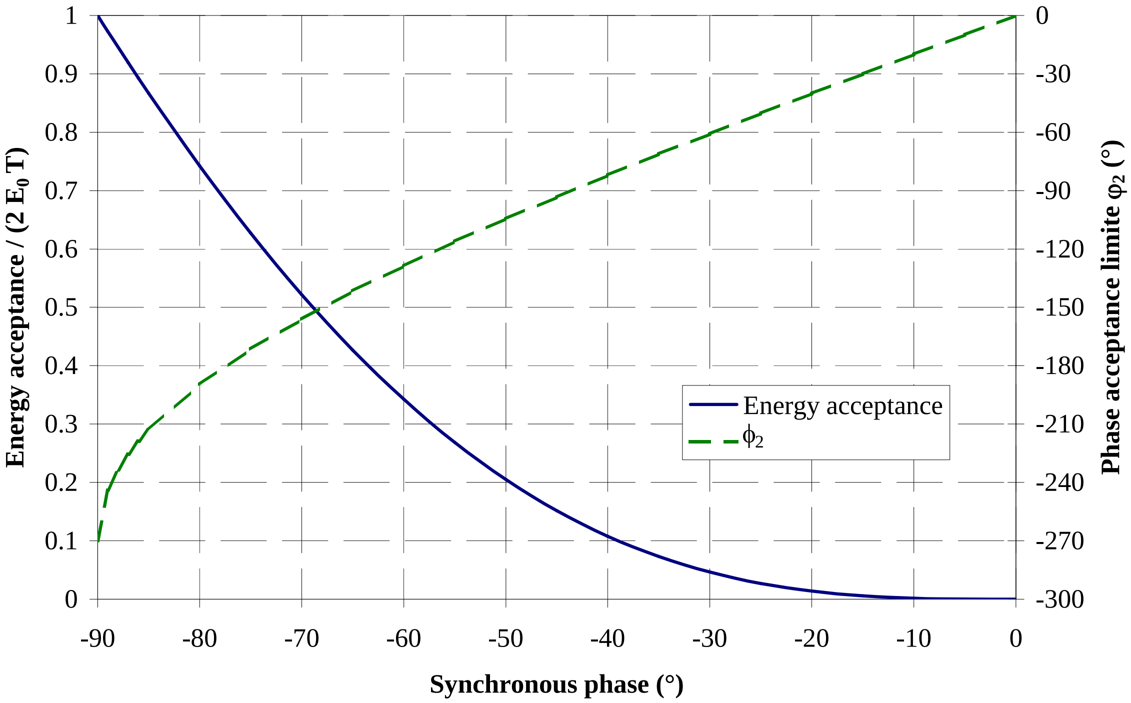

Figure 7 : Bucket dimensions as a function of the synchronous phase

For small phase amplitude oscillations, equations **(63)** becomes:

$$\begin{cases} \dfrac{d\varphi}{ds} = -2\pi \cdot \dfrac{w}{(\beta_s\gamma_s)^3 \cdot mc^2 \cdot \lambda} \\ \dfrac{dw}{ds} = q \cdot E_0 T_s \cdot \sin\phi_{s0} \cdot \varphi \end{cases} \quad \textbf{(71)}$$

giving the second order differential equation of phase evolution:

$$\frac{d^2\varphi}{ds^2} + \frac{2}{\varsigma} \cdot \frac{d\varphi}{ds} + k_z^2 \cdot \varphi = 0 \quad \textbf{(72)}$$

with:

- $$k_z^2 = \frac{2\pi q \cdot E_0 T_s \cdot \sin(-\phi_{s0})}{(\beta_s\gamma_s)^3 \cdot mc^2 \cdot \lambda}. \quad \textbf{(73)}$$

  k_z is the phase advance per meter of the beam core. In periodic structures of period L, $\sigma_z = k_z L$ is the longitudinal core phase advance per lattice.

- $$\varsigma = \frac{2}{3} \cdot \frac{\beta_s\gamma_s}{d(\beta_s\gamma_s)/ds}. \quad \textbf{(74)}$$

  ς is the damping length of the core oscillations.

Both ς and the variation of k_z with $\beta_s\gamma_s$ contribute to phase oscillation damping with acceleration. The adiabatic damping of the phase amplitude oscillation $\boldsymbol{\varphi_a}$, defined when the contribution of ς is negligible, can be calculated [6]:

$$\varphi_a \propto (\beta_s\gamma_s)^{-3/4}. \tag{75}$$

Liouville theorem implies that the energy amplitude oscillation $\boldsymbol{w_a}$ variation is:

$$w_a \propto (\beta_s\gamma_s)^{3/4}.$$

The Hamiltonian in linear force becomes then:

$$H_{\varphi w} = -\frac{2\pi}{(\beta_s\gamma_s)^3 \cdot mc^2 \cdot \lambda} \cdot \frac{w^2}{2} + q \cdot E_0 T_s \cdot \sin\phi_{s0} \cdot \frac{\varphi^2}{2} \tag{76}$$

The curves for which the Hamiltonian is constant are then ellipses.

4.5 Motion in linear force

We have seen that the longitudinal particle motion is basically non linear, but it can be linearised when the particle phase oscillation amplitude is very small compared to ϕ_l. The transverse forces are much more linear than the longitudinal one, and the use of linear focusing force is very close to the reality, and can be solved analytically.

4.5.1 Linear transverse forces

In linacs, the main elements used to transport a beam are the cavities and the quadrupoles. These both elements induce transverse forces.

Quadrupoles

In perfect thick lens quadrupole the magnetic field is:

$$\begin{cases} B_x = G \cdot y \\ B_y = G \cdot x \end{cases} \tag{77}$$

G is the quadrupole gradient (in T/m).

With the paraxial approximation and because magnetic field does not change the particle energy, the equations of transverse dynamics in quadrupole are then:

$$\begin{cases} \dfrac{d\gamma\beta_x}{ds} = \gamma\beta_z \dfrac{dx'}{ds} = -\dfrac{q \cdot G}{mc} x \\ \dfrac{dx}{ds} = x' = \dfrac{\beta_x}{\beta_z} \\ \dfrac{d\gamma\beta_y}{ds} = \gamma\beta_z \dfrac{dy'}{ds} = \dfrac{q \cdot G}{mc} y \\ \dfrac{dy'}{ds} = y' = \dfrac{\beta_y}{\beta_z} \end{cases} \tag{78}$$

The transverse perfect quadrupole force is linear.

Actually, fringe field and non-perfect hyperbolic poles induce non linear effects which can be generally neglected at first order in linacs.

RF gap

When a particle travels through a cavity, the integration of the effect of the radial electric field and the azimuthal magnetic field can be modelised by a transverse kick, which is linear at second order. This kick modifies the particle transverse momentum:

$$\Delta(\gamma\beta_r) = -\frac{\pi q E_0 T L}{mc^2 \overline{\gamma\beta_z}^2 \lambda} \cdot \sin\phi \cdot \left(r + O\left(r^3\right)\right) = \Delta(\gamma\beta_z) \cdot r' + \gamma\beta_z \cdot \Delta r' . \tag{79}$$

With $\beta_r^2 = \beta_x^2 + \beta_y^2$.

The term in *r'* shows that the particle transverse oscillation is damped by acceleration in accelerating cavities.

4.5.2 Motion of particle in periodic linear force

At first order, the motion of particle can be linearised and the motion along all directions can be decoupled. The motion equation in *w* direction (*w* being *x*, *y* or φ) is solution of a second order equation:

$$\frac{d^2 w}{ds^2} + \frac{A_w}{\gamma\beta_z} \cdot \frac{d\gamma\beta_z}{ds} \cdot \frac{dw}{ds} + k_w(s) \cdot w = 0 . \tag{80}$$

A_w being a constant equal to 1 for $w = x$ or y and 3 for $w = \varphi$.

Now, lets consider that the focusing force is periodic with period ***S***, i.e.: $k_x(s+S) = k_x(s)$.

Generally, the damping term given by the acceleration is very small and can be considered as a perturbation:

$$\left\langle \frac{A_w}{\gamma\beta_z} \cdot \frac{d\gamma\beta_z}{ds} \cdot \frac{dw}{ds} \right\rangle_S << \left\langle k_w(s) \cdot w \right\rangle_S , \tag{81}$$

$\langle a \rangle_S$ giving the average value of quantity *a* over one lattice period.

In this assumption, the solution of equation **(80)** is:

$$w(s) = \sqrt{\beta_{wm}(s) \cdot I_w / \gamma\beta_z} \cdot \cos\left(\psi_w(s - s_0) + \psi_w(s_0)\right), \tag{82}$$

with $\boldsymbol{\beta_{wm}}$ periodic ($\beta_{wm}(s+S) = \beta_{wm}(s)$), known as the structure beta function, solution of:

$$\frac{d^2\beta_{wm}}{ds^2} + 2 \cdot k_w(s) \cdot \beta_{wm} - \frac{2}{\beta_{wm}} \cdot \left(1 + \frac{1}{4} \cdot \left(\frac{d\beta_{wm}}{dt}\right)^2\right). \tag{83}$$

$I_w / \gamma\beta_z$, known as the *Courant-Snyder* invariant (which is actually invariant with no acceleration), and ψ_w the particle phase advance, defined as:

$$\psi_w(s)=\int_{s_0}^{s}\frac{ds}{\beta_{wm}(s)}. \quad \textbf{(84)}$$

Particles are turning around periodic ellipses whose equations are:

$$\gamma_{wm}(s)\cdot w^2+2\cdot\alpha_{wm}(s)\cdot w\cdot w'+\beta_{wm}(s)\cdot w'^2=I_w/\gamma\beta_z\ , \quad \textbf{(85)}$$

$$\text{with: } \alpha_{wm}(s)=-\frac{1}{2}\frac{d\beta_{wm}(s)}{ds}, \quad \textbf{(86)}$$

$$\text{and: } \gamma_{wm}(s)=\frac{1+(\alpha_{wm}(s))^2}{\beta_{wm}(s)}. \quad \textbf{(87)}$$

The surface of the ellipses is decreasing as $1/\gamma\beta_z$ which is close to $1/\gamma\beta$ with the paraxial approximation.

The *phase advance per lattice* σ_w defined as:

$$\sigma_w=\psi_w(s+S)-\psi_w(s), \quad \textbf{(88)}$$

gives an idea of how fast the particles are turning around the ellipses. The number $\frac{2\pi}{\sigma_w}$ is the number of lattice periods after which the particle has made one turn around the ellipses. One can notice that, in linear forces, the phase advance per lattice is the same whatever the particle amplitude.

As an example, let have a look on a particle motion along one direction in a FODO channel. On **Figure 8**, 5 FODO lattices have been represented.

The particle phase advance per lattice is 360°/5=72°. The particle position in 2D phase-space is represented by the red point in 4 different positions in the lattice. Each line correspond to one position:

1rst line: middle of focusing quadrupole,

2nd line: between focusing and defocusing quadrupoles,

3rd line: middle of defocusing quadrupole,

4th line: between defocusing and focusing quadrupoles.

One observes that lattice after lattice, at the same position, the particle turns around an ellipse. The ellipse is different from position to position within the lattice. Its equation is given by **(85)**. This is very important to figure out that these ellipses have nothing to do with the beam (no beam have been defined here, but just one particle). These ellipses are defined by the transport channel only.

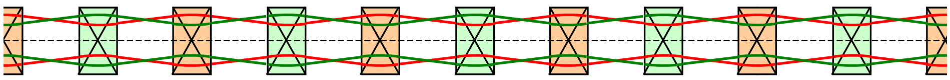

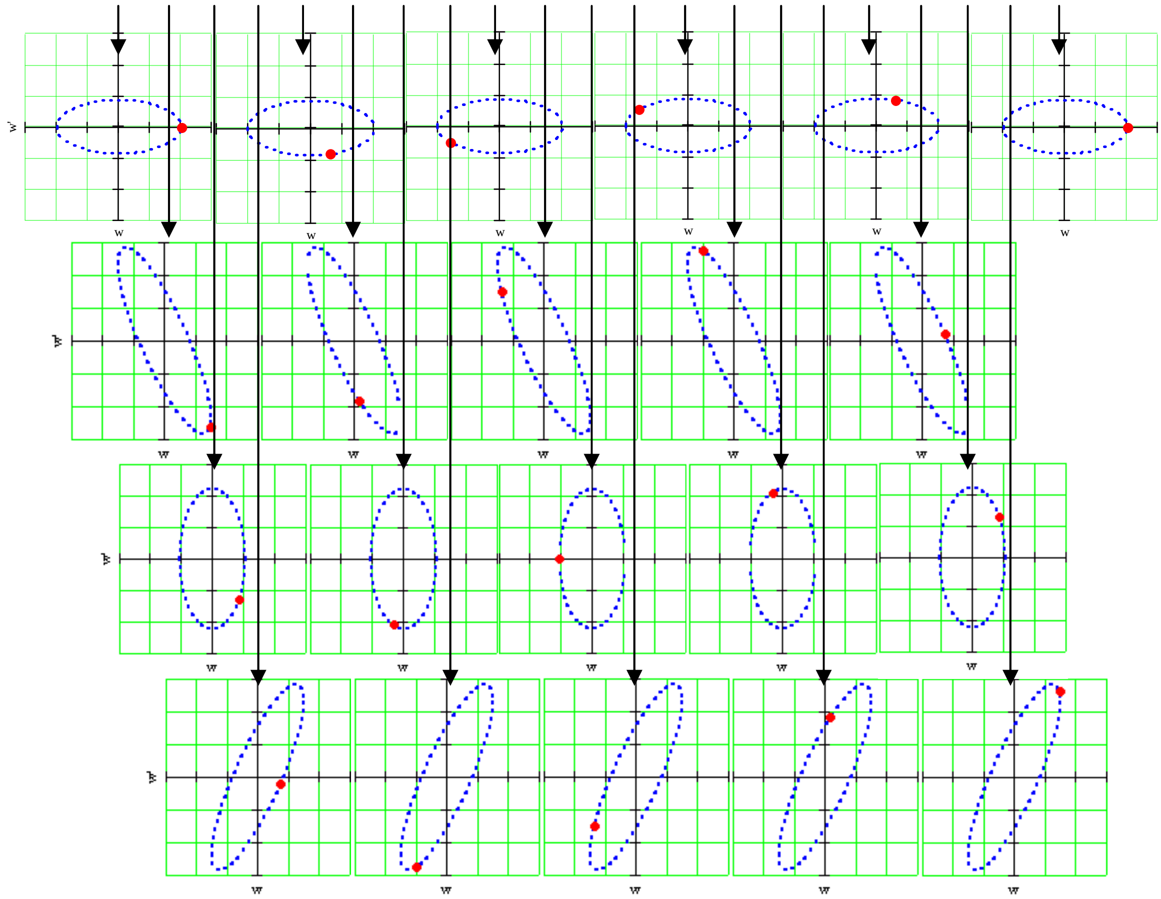

Figure 8 : Particle transport in a FODO channel

As a conclusion, we should keep in mind that a large number of assumptions have been done to get that results. The opportunity of each assumption has to be studied very carefully in practical cases. Nevertheless, the results presented here give a good understanding of the beam dynamics.

4.6 Beam RMS dimension and Twiss parameters

A bunch is constituted of N particles. Its dimensions can be are defined statistically as followed:

- The beam centre of gravity position: $\langle w \rangle = \dfrac{1}{N} \sum\limits_{i=1,N} w_i$, **(89)**

- The beam centre of gravity slope: $\langle w' \rangle = \dfrac{1}{N} \sum\limits_{i=1,N} w'_i$, **(90)**

- The beam RMS size: $\tilde{w} = \sqrt{\left\langle \left(w - \langle w \rangle\right)^2 \right\rangle} = \sqrt{\dfrac{1}{N} \sum\limits_{i=1,N} \left(w_i - \langle w \rangle\right)^2}$, **(91)**

- The beam RMS divergence: $\tilde{w}' = \sqrt{\left\langle \left(w' - \langle w' \rangle\right)^2 \right\rangle} = \sqrt{\dfrac{1}{N} \sum\limits_{i=1,N} \left(w'_i - \langle w' \rangle\right)^2}$, **(92)**

- The beam RMS emittance: $\tilde{\varepsilon}_w = \sqrt{\tilde{w}^2 \tilde{w}'^2 - \langle (w - \langle w \rangle) \cdot (w' - \langle w' \rangle) \rangle^2}$. **(93)**

The beam *Twiss parameters* are then deduced from the beam rms dimensions:

$$\tilde{\beta}_w = \frac{\tilde{w}^2}{\tilde{\varepsilon}_w}, \qquad \tilde{\gamma}_w = \frac{\tilde{w}'^2}{\tilde{\varepsilon}_w}, \qquad \tilde{\alpha}_w = -\frac{\langle (w - \langle w \rangle) \cdot (w' - \langle w' \rangle) \rangle}{\tilde{\varepsilon}_w}. \tag{94}$$

Generally, at least 90% of the bunch particles occupy an ellipse of equation[10]:

$$\tilde{\gamma}_w \cdot w^2 + 2 \cdot \tilde{\alpha}_w \cdot w \cdot w' + \tilde{\beta}_w \cdot w'^2 = 5 \cdot \tilde{\varepsilon}_w. \tag{95}$$

The parameter w can be x, y, z or φ. On **Figure 9** is represented the phase-space 2D projections of a beam with ~100,000 particles. Ellipses in red correspond to ellipses calculated with equation **(95)**. They contain, in this example, 92% of the particles.

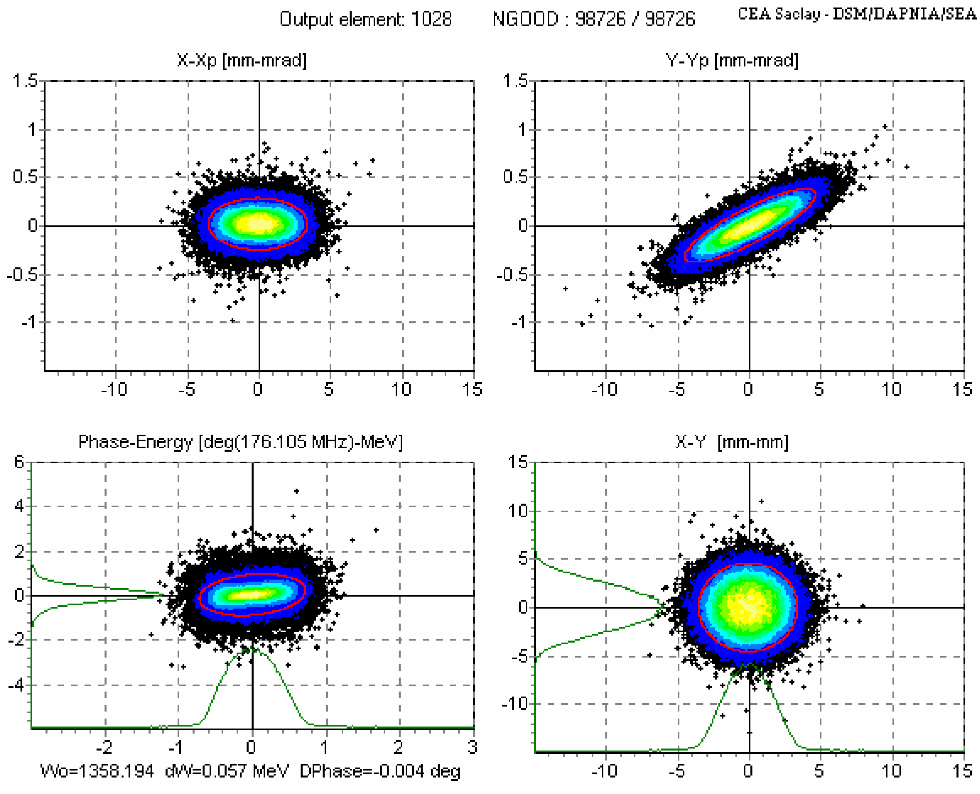

Figure 9 : Phase-space beam distribution and Twiss parameters

4.7 Matched/Mismatched beam

A beam is matched when its Twiss parameters at a given position s correspond to the transport channel periodic Courant-Snyder parameters. In this condition, the same beam phase-space shape is reproduced period after period. The envelope evolution with s is periodic and the smoothest as possible. On **Figure 10** has been represented the evolution of beams in the same FODO channel as

[10] If the bunch was uniform, 100% of the particles would occupy this ellipse.

before (upper line). In the middle line are represented the ellipses represented the beams in the phase-space at the focusing quadrupole centre. The dashed black circle represents a particle motion in this channel. One matched (in continuous red) and two mismatched (in dashed pink and dotted blue) beams have been represented. One particle of each beams have also been represented.

The matched beam ellipse is periodic, as one particle is replaced by an other one. Its envelope (last line) is periodic with the lattice period ***L***.

The mismatched beam ellipses are sweeping an bigger area (dashed-black circle) than the beam ellipse surfaces. Their envelopes period is greater than the lattice period. Its oscillation is a combination of two oscillations with two different periods: one is the lattice period *L*, the other is $2\pi/\sigma_w \cdot L$, σ_w being the channel phase advance per lattice.

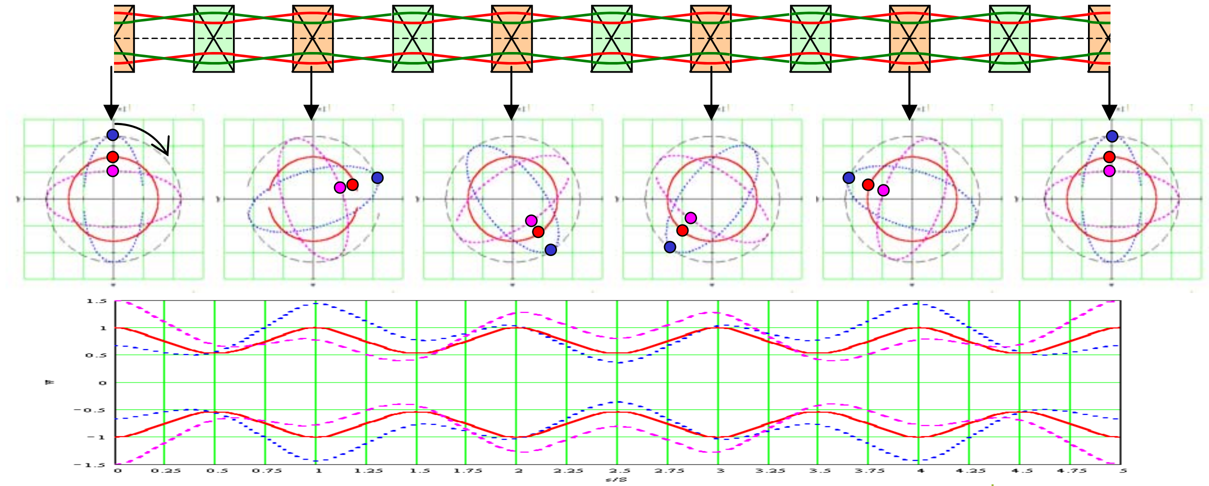

Figure 10 : Matched and mismatched beam in FODO channel

- When the <u>force is linear</u> (**Figure 11**), all particles are turning in the phase-space with the same period (i.e. the same phase advance per lattice). The beam phase-space distribution is changing lattice after lattice, but its emittance is kept constant.

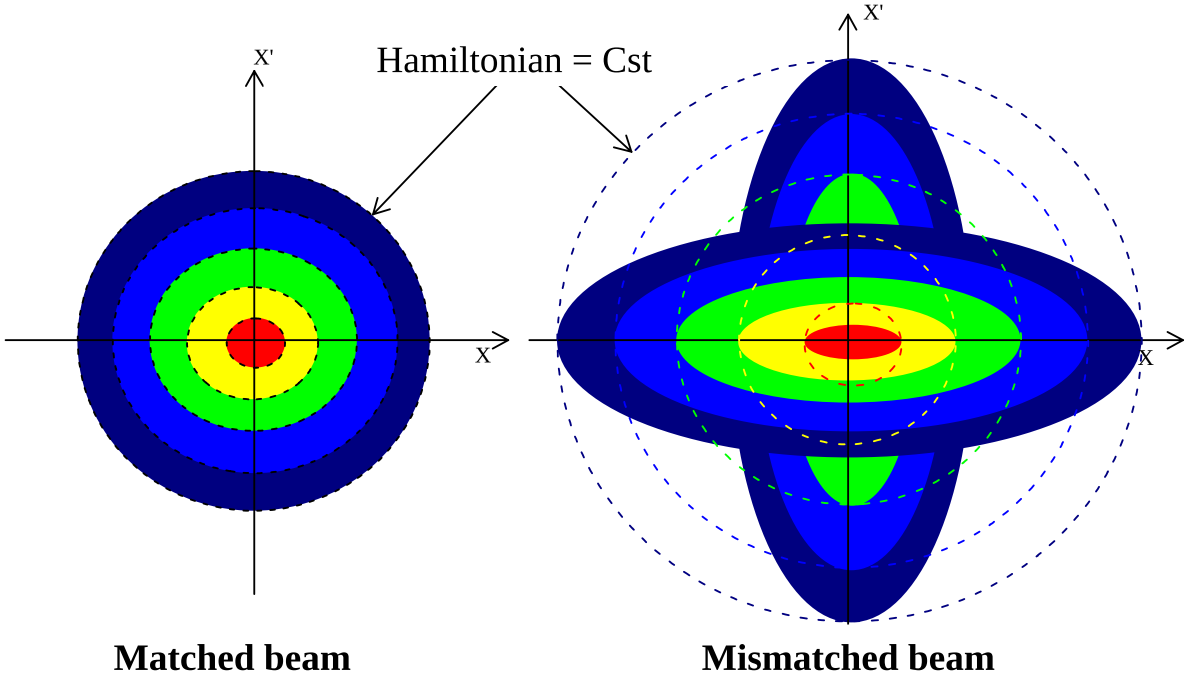

Figure 11 : Matched (left) and mismatched (right) beam in linear forces

- When the force is non linear (**Figure 13**) (external force or force induced by space-charge (coulombian interactions between beam particles)), particle phase-advance per lattice depends on its oscillation amplitude. Beam particles are no more turning all at the same speed, and an apparent emittance growth is observed[11]. This effect is known as the beam filamentation (**Figure 12**). After a long time (many particle betatron periods), the phase-space swept by the beam is completely full of particle. The apparent emittance is larger.

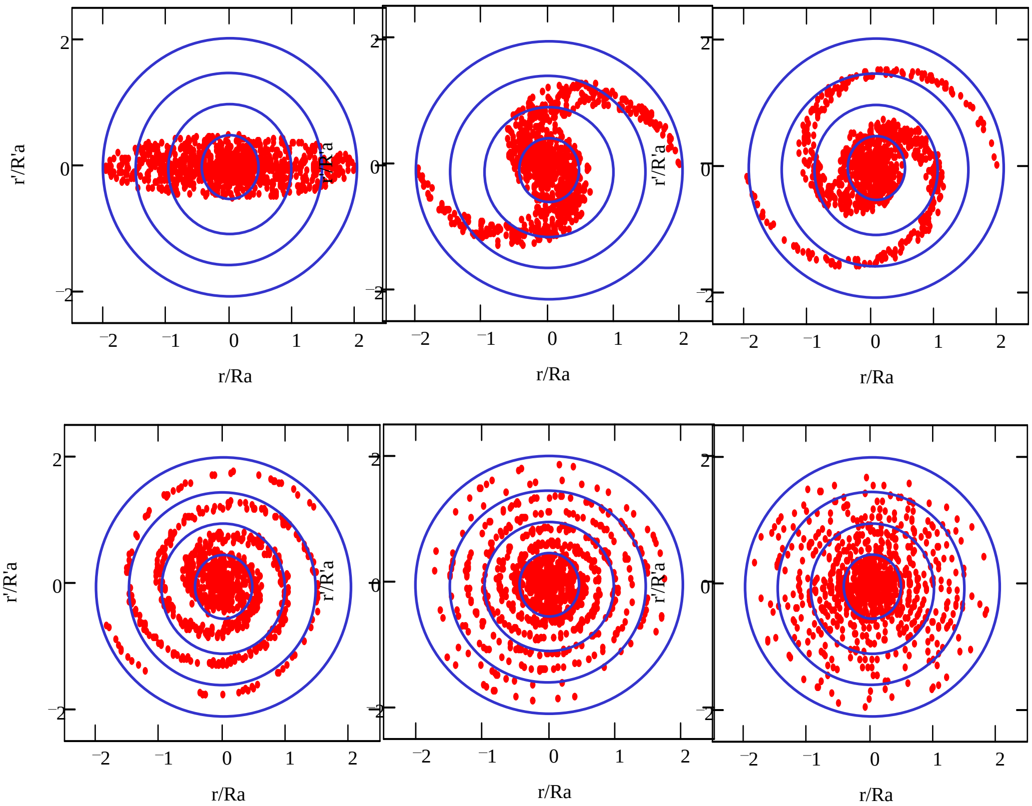

Figure 12 : Filamentation of mismatched beam in non linear force

[11] Even if the phase-space area occupied by the particle is constant (Liouville theorem applies).

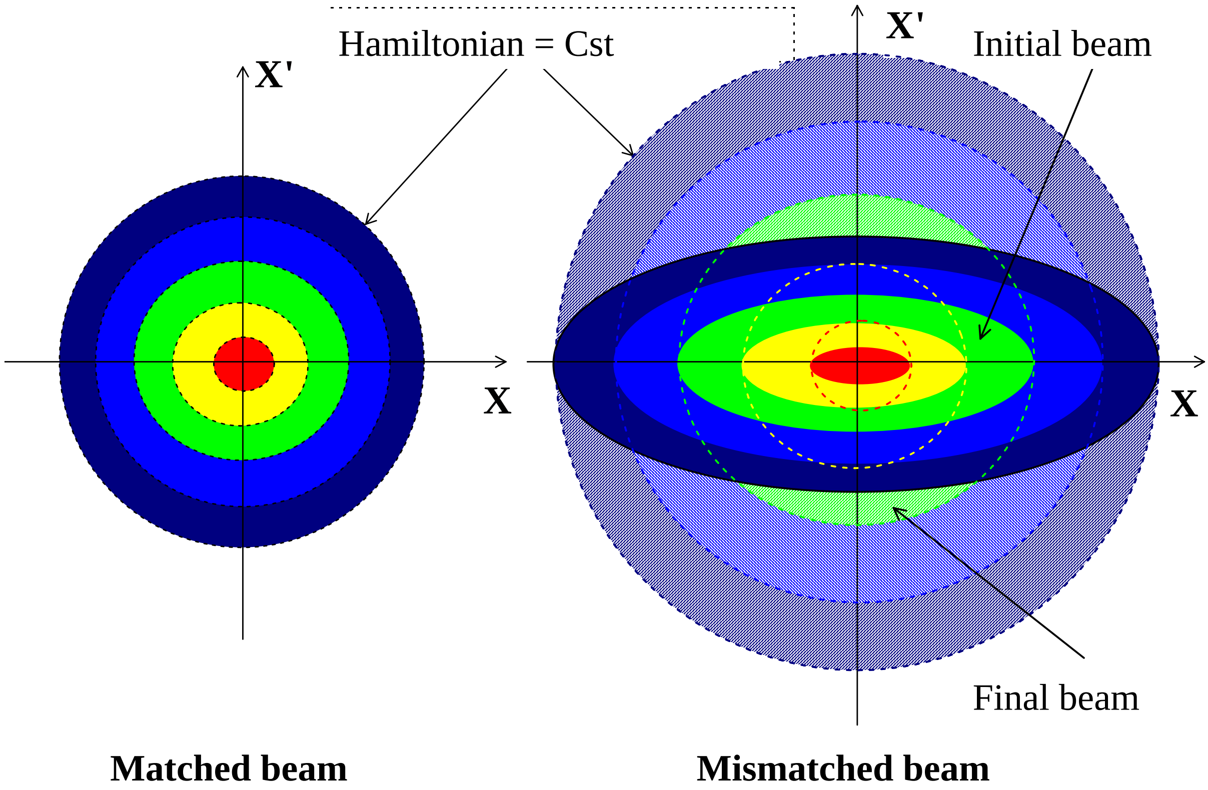

Figure 13 : Matched (left) and mismatched (right) beam in non linear forces

5. CONCLUSION

This paper is a short introduction containing the first basic notions useful for a first approach with linacs. A better understanding cannot be obtained without tackling subjects like the existing structures, the RF control, the space-charge effects or the resonances. Motivated students are strongly advised to read tom Wangler's book [2].

6. ACKNOWLEDGEMENTS

Many thanks to Tom Wangler for its wonderful and very useful book on linacs and his encouragement and to my colleagues Romuald Duperrier and Didier Uriot for their help.

REFERENCES

[1] *Linear Accelerators*, Lapostolle & Septier Editors, 1970.

[2] T. Wangler, *RF Linear Accelerators*, Wiley & sons ed, 1998.

[3] *RF engineering for particle accelerators*, CERN Accelerator School, Oxford, UK, 3-10 April 1991.

[4] T. Nishikawa, "Transients and Beam Loading Effect", *Linear Accelerators*, Lapostolle & Septier Editors, 1970.

[5] Mario Weiss, "Introduction to RF linear Accelerators", *CAS*, fifth general accelerator physics course, Jyväskylä, Finland, 7-18 September 1992.

[6] A. Carne et al., "Numericals methods. Acceleration by a gap", *Linear Accelerators*, Lapostolle & Septier Editors, 1970.

[7] J. Le Duff, "Dynamics and acceleration in linear structures", *Fifth general accelerator physics course,* CERN Accelerator School, Jyväskylä, Finland, 7-18 September 1992.